Supramolecular Chemistry

DOI: 10.1002/ange.200600847

Molecular Self-Assembly of Macroporous Parallelogrammatic Pipes**

*Myungeun Seo, Gon Seo, and Sang Youl Kim**

Controlling the shape and symmetry of supramolecular materials is essential to express the desired functionalities of new materials. Most self-assembled materials have spherical or cylindrical morphologies, because soft amphiphilic molecules tend to aggregate to form spheres, which are the most thermodynamically stable shape.[1] Consequently, the generation of unique shapes with lower symmetries in self-assembled soft materials has been limited. We aimed to develop a strategy to control the shape and symmetry of the self-assembled materials by a taking two-step approach: First,

[*] M. Seo, Prof. S. Y. Kim
Department of Chemistry and School of Molecular Science (BK21)
Korea Advanced Institute of Science and Technology
373-1 Guseong-dong, Yuseong-gu, Daejeon, 305-701 (Korea)
Fax: (+82) 42-869-8177
E-mail: kimsy@kaist.ac.kr
Homepage: http://macro.kaist.ac.kr
Prof. G. Seo
School of Applied Chemical Engineering & The Research Institute for Catalysis
Chonnam National University
300 Yongbong-dong, Buk-gu, Gwangju, 500-757 (Korea)

[**] Financial support by the BK 21 program and by the Basic Research Program of the KOSEF (grant number R01-2006-000-11258-0) is acknowledged. The authors thank J. Lee for X-ray crystallography, Prof. C. Shin for CP-MAS ^{13}C NMR measurements and porosity evaluation, and Prof. T. Hayakawa and Photron Ltd. for the real-time imaging of the pipe growth.

Supporting information for this article is available on the WWW under http://www.angewandte.org or from the author.

polymorphic molecular aggregates were constructed with highly directed noncovalent bonds and second, the evolution process was controlled by applying nonequilibrium conditions during the self-assembly.[2] As an example to show the potential of our strategy, we demonstrate the formation of hollow parallelogrammatic pipes through simple drying-mediated self-assembly of organic molecules.

We designed a molecular aggregate based on the hydrogen-bonded network of primary aromatic amides to achieve a parallelogrammatic shape. Primary aromatic amides are known to form 2-dimensional hydrogen-bonded networks through highly directional side-to-side and face-to-face hydrogen bonds involving anti (H_{anti}) and syn protons (H_{syn}), respectively.[3,4] In the present work, we synthesized 4-dodecyloxy-2-trifluoromethylbenzamide (**1**, Figure 1a),

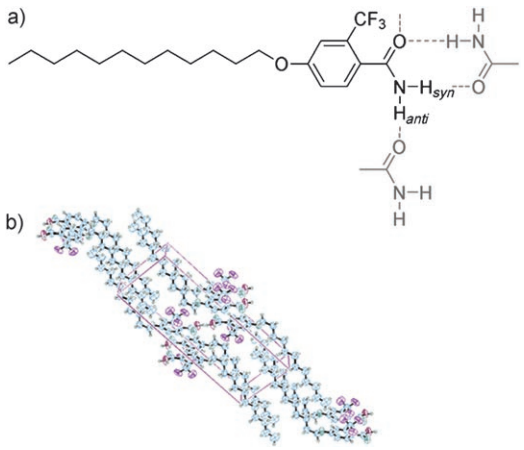

Figure 1. a) Molecular structure and hydrogen bonding pattern of **1**. b) ORTEP drawing of the crystal structure of **1L**.

which is highly crystalline as a result of the interaction between lipophilic alkyl chains and the strong hydrogen bonds. Compound **1** shows polymorphism: two different crystal structures were identified in the powder X-ray diffraction (XRD) patterns. The crystallization of **1** from *n*-hexane and solidification of the melt yielded a needlelike crystal with a small-angle peak at $d = 2.39$ nm (**1L** structure), whereas the crystallization in polar solvents such as ethanol, ethyl acetate, acetone, and diethyl ether produced rodlike crystals with a small-angle peak at $d = 1.48$ nm (**1S** structure).

The triclinic unit cell of the **1L** structure, obtained from the single crystal grown in *n*-hexane, is illustrated in Figure 1b.[5] The molecules form an intercalated head-to-head bilayer structure, and the primary amide groups form a hydrogen-bonded network that consists of side-to-side and face-to-face hydrogen bonds in the layer.

However, we were unable to grow a suitable single crystal of the **1S** structure. In ethanol, a powder precipitated at low concentration and the solution became a crystalline gel at concentrations greater than 15% w/v (see the Supporting Information). Thus we assumed that the **1S** structure is triclinic and assigned the three crystallographic axes as $a = 0.725$, $b = 1.13$, and $c = 1.48$ nm on the basis of the powder XRD pattern. Compared with the **1L** structure, the supposed unit cell has a considerably shorter c axis even though its volume is similar to that of the **1L** structure. This observation suggests that the alkyl chains in the **1S** structure are more disordered than those in the **1L** structure. ^{13}C cross-polarization magic-angle-spinning (CP-MAS) solid-state NMR spectra and FT-IR spectra reveal a large fraction of gauche conformations,[6,7] and a large red shift of the N–H symmetric stretching vibration to 3184 cm^{-1} (3196 cm^{-1} in the **1L** structure) indicates that the face-to-face hydrogen bond of the **1S** structure is much stronger than that of the **1L** structure (see the Supporting Information).[4a] These spectroscopic data suggest that the strong face-to-face hydrogen bond stabilizes the **1S** structure, whereas the rapid crystallization of the alkyl chains favors the **1L** structure. The fact that the **1S** structure grows only in polar solvents can be rationalized by the solvation of the H_{syn} atom by an O atom of the solvent molecule.

To utilize the difference between two polymorphs in the assembly, we irreversibly evaporated a solution of **1** in a polar solvent. Evaporation from a drop of solution on a substrate is a complex nonequilibrium process.[8,9b] The possibility of using evaporation to produce unique two-dimensional supramolecular patterns on a mesoscopic scale has been exploited recently.[8–12]

We found that evaporation resulted in unusual crystal growth when a hot solution of **1** in polar solvents was allowed to drop onto a substrate. In a typical experiment, a solution of **1** in ethanol at 96 °C was allowed to drop onto a silicon wafer at room temperature. The process of the structure evolution was imaged in real time by an optical microscope (a movie clip is available in the Supporting Information). Figure 2a

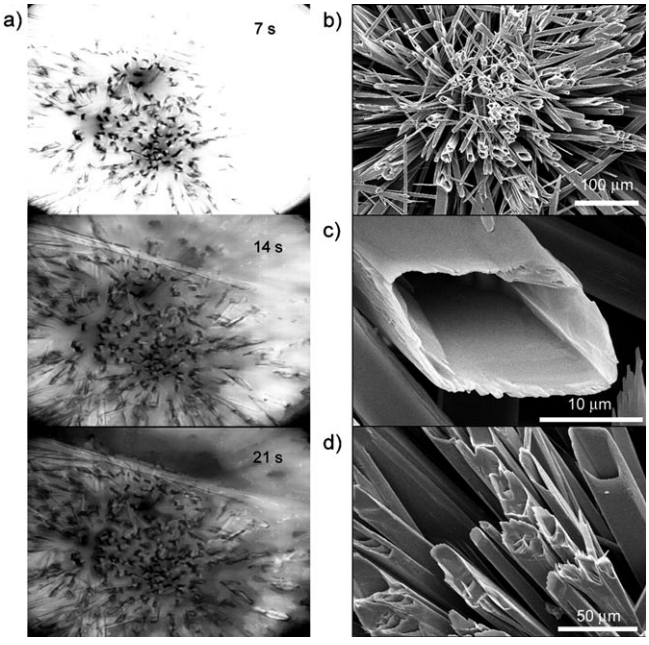

Figure 2. Drying-mediated assembly of **1** to generate a bundle of pipes: a) Snapshots of the pipe formation during the evaporation. The sample was prepared by allowing a hot solution of **1** (20% w/v) in ethanol to drop onto a silicon wafer at room temperature. The time lapse after the solution was dropped is given in the top left of each picture. b-d) SEM images of: b) a macroscopic view of the hemispherically formed pipes; c) an enlarged view of a typical pipe; d) some partitioned pipes.

shows three snapshots taken during the process. As ethanol evaporated, rodlike crystals nucleated at the surface of the drop and grew inside to form three-dimensional hemispherical bundles. Field-emission scanning electron microscopy (FE-SEM) images show that bundles of micrometer-sized parallelogrammatic pipes were formed (Figure 2b–d). The pipes were about 1 mm high, and the cross section was about $20 \times 15\ \mu m^2$ with angles of 80 and 100°. The thickness of the wall was about 150 nm. Although most pipes were parallelogrammatic, some of the pipes consisted of more-complex shapes; platelike crystals were observed in regions around the bundle. The growth was completed within one minute.

Figure 3a depicts the powder XRD patterns of the solids that remained on the wafer. Series of peaks were assigned to the **1L** and **1S** structures. However, the pattern obtained from carefully selected pipes consisted almost solely of the **1L** structure (Figure 3b). Because the crystallization in ethanol yielded only the **1S** structure, the **1L** structure should be generated during the evaporation, when the alkyl chains crystallize rapidly. Indeed, dropping a hot solution of **1** in ethanol onto a silicon wafer at 96 °C yielded the **1L** structure.

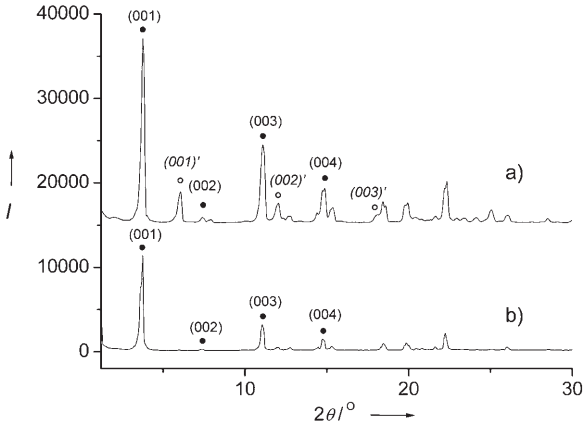

Figure 3. Powder XRD patterns of **1** formed on the silicon wafer: a) The whole solid after the complete evaporation. b) Carefully selected pipes. Filled circles: Bragg peaks with the spacing of 2.40 nm. Open circles: Bragg peaks with the spacing of 1.48 nm.

We believe that the polymorphic transition of **1S** into **1L** during the evaporation is crucial in the formation of the unusual parallelogrammatic cross section of micrometer size. The formation of parallelogrammatic channels can not be explained by the bent backbone in the crystal structure because this backbone is restricted to within the nanometer scale.[13a] Some reports regard one-dimensional growth in the liquid crystalline (LC) medium and the filling of the cavity with LC fluid as a key mechanism in the formation of micrometer-sized tubes.[13b,c] However, the resulting tubes are highly symmetric (hexagonal), and the growth process is surprisingly slow relative to the present result. Thus, we suggest a different mechanism, which involves the transition between two polymorphs to give the self-templated hollow structure. Figure 4 summarizes the main features of this mechanism. A similar mechanism that involves organic crystals as templates in the formation of hollow fibers with parallelogrammatic cross section has been proposed.[14]

The whole drop is a dynamic system in which a Benárd convective flow occurs owing to the temperature difference between the surface and the bottom fo the drop.[8] This flow transports hot solution from the bottom toward the colder surface of the drop. The solution becomes saturated, and solvent-rich gel-like solid of **1S** structure forms. However, when the solid comes in contact with air during the evaporation, the rapid crystallization of alkyl chains induces the **1L** structure instantaneously and creates a wall around the gel-like solid. Then, solute flows toward the wall to compensate the solute consumed by crystallization of the **1L** structure. The concentration inside the wall decreases continuously as a result of consumption of the solute. Consequently, the solvent evaporates and leaves a parallelogrammatic channel resembling the shape of the **1S** crystal. The radial-bundle shape can be attributed to the radial convective flow. Platelike crystals of **1L** structure at the boundary of the droplet may appear because of the small temperature difference between the surface and the bottom of the drop. Residual **1S** structure may crystallize inside the drop near the bottom without the contact to air. To verify this hypothesis, we measured the powder XRD of a sample immediately quenched with liquid nitrogen after the dropping of the solution. The data show that the **1S** structure appears in high population at a very early stage of the growth process, which

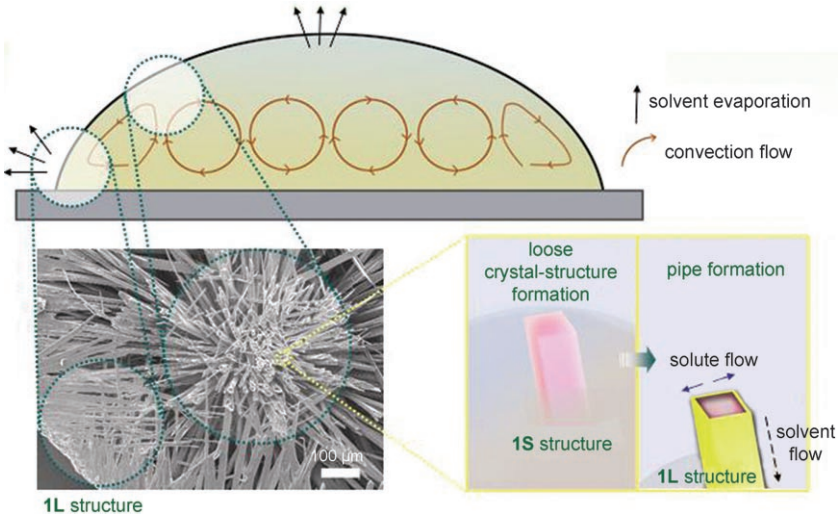

Figure 4. The proposed mechanism of pipe formation based on the polymorphic transition: The **1L** structure forms at the boundary of the droplet as a result of evaporation. Benárd convective flow around the center of the drop induces crystallization of the **1S** structure near the surface of the droplet. However, polymorphic transition from the **1S** to the **1L** structure yields a crystalline wall, the inside of which is hollow because of solute flow to the wall to compensate for the consumption of solute upon crystallization.

supports the proposed mechanism (see the Supporting Information).

This organic supramolecular material can be regarded as a new type of macroporous material. We confirmed the existence of the macropores by using a mercury intrusion porosimeter (Figure 5a). The result shows the development

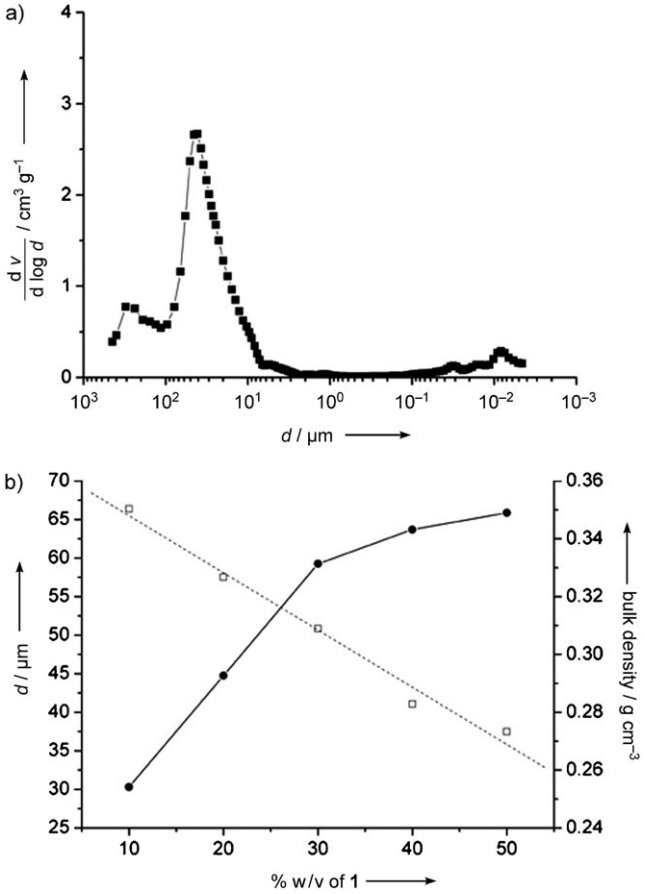

Figure 5. a) Typical pore-size distribution of the pipes. The sample was prepared from a 40% w/v solution in ethanol. Porosity: 73%. Maximum mean pore diameter: 41.1 µm. b) Plot of content (% w/v) of **1** in ethanol versus maximum mean pore diameter and bulk density of the pipes. Filled dots: bulk density. Empty squares: maximum pore diameter. Dashed line: least-squares fit of maximum pore diameter plot ($R = 99.2\%$).

of pipes with the average pore diameter of tens of micrometers, which corresponds to those observed by SEM. The average pore diameter of the pipes was gradually reduced with increases of the concentration of **1** (Figure 5b), which indicates that it is possible to tune the pore size.

In summary, we developed a novel self-templating technique between polymorphs and demonstrated the formation of organic macroporous parallelogrammatic pipes through drying-mediated assembly. We expect that this strategy to generate organic materials with lower symmetries in a macroscopic dimension will open a route to develop hollow macroscopic structures with unusual shapes.

Experimental Section

The detailed synthesis of **1** is provided in the Supporting Information. To generate parallelogrammatic pipes, 20% w/v solution of **1** in ethanol was prepared at 96°C and allowed to drop onto a silicon wafer that had been freshly washed with piranha solution. The drop was allowed to evaporate at RT. The process of the structure evolution was imaged by a Nikon ME600L microscope equipped with a Photron Focuscope all-in-focus system. FE-SEM studies were performed on Philips XL30S FE-SEM for Au-sputtered samples. Powder XRD patterns were obtained on Rigaku D/MAX Ultima diffractometer with scan speed of 2° min^{-1}, sampling width of 0.01°, and $Cu_{K\alpha}$ ($\lambda = 0.154$ nm) as a light source. Mercury porosimetry isotherms were obtained with an AutoPore III (Micromeritics). The samples were evacuated under vacuum (below 3×10^{-2} Torr) at room temperature prior to intrusion of mercury. The Kelvin equation was used to determine the pore-size distribution of the samples. The contact angle between sample and mercury was chosen as 140°.

Received: March 5, 2006
Revised: July 2, 2006
Published online: August 29, 2006

Keywords: crystal growth · polymorphism · self-assembly · X-ray diffraction

[1] T. Kunitake, Y. Okahata, M. Shimomura, S. Yasunami, K. Takarabe, *J. Am. Chem. Soc.* **1981**, *103*, 5401–5413; H.-A. Klok, S. Lecommandoux, *Adv. Mater.* **2001**, *13*, 1217–1229.

[2] G. M. Whitesides, B. Grzybowski, *Science* **2002**, *295*, 2418–2421; G. M. Whitesides, M. Boncheva, *Proc. Natl. Acad. Sci. USA* **2002**, *99*, 4769–4774.

[3] M. C. Etter, *Acc. Chem. Res.* **1990**, *23*, 120–126; M. C. Etter, *J. Phys. Chem.* **1991**, *95*, 4601–4610.

[4] a) L. S. Reddy, A. Nangia, V. M. Lynch, *Cryst. Growth Des.* **2004**, *4*, 89–94; b) C. M. Reddy, L. S. Reddy, S. Aitipamula, A. Nangia, C.-K. Lam, T. C. W. Mak, *CrystEngComm* **2005**, *7*, 44–52.

[5] Crystal data for **1L**: $C_{20}H_{30}F_3NO_2$, triclinic, space group $P\bar{1}$, scan range $3.4 < 2\theta < 56.3°$, $T = 293(2)$ K, $a = 4.9837(13)$, $b = 8.952(2)$, $c = 23.931(6)$ Å, $\alpha = 93.495(5)$, $\beta = 90.810(5)$, $\gamma = 93.460(5)°$, $V = 1063.5(5)$ Å^3, $Z = 2$, $\rho_{calcd} = 1.166$ g cm^{-3}, $\mu(Mo_{K\alpha}) = 0.092$ mm^{-1}, 12062 unique reflections, of which 4746 were taken as observed [$I > 2\sigma(I)$], $R\,|\,F^2\,| = 0.2093$, $wR = 0.1397$. CCDC-600374 contains the supplementary crystallographic data for this paper. These data can be obtained free of charge from The Cambridge Crystallographic Data Centre via www.ccdc.cam.ac.uk/data_request/cif.

[6] M. Pursch, R. Brindle, A. Ellwanger, L. C. Sander, C. M. Bell, H. Handel, K. Albert, *Solid State Nucl. Magn. Reson.* **1997**, *9*, 191–201.

[7] M. Matsuda, V. Volkmar, T. Shimizu, *J. Am. Chem. Soc.* **2000**, *122*, 12327–12333.

[8] M. Shimomura, T. Sawadaishi, *Curr. Opin. Colloid Interface Sci.* **2001**, *6*, 11–16.

[9] a) A. P. H. J. Schenning, F. B. G. Benneker, H. P. M. Geurts, X. Y. Liu, R. J. M. Nolte, *J. Am. Chem. Soc.* **1996**, *118*, 8549–8552; b) M. C. Lensen, K. Takazawa, J. A. A. W. Elemens, C. R. L. P. N. Jeukens, P. C. M. Christianen, J. C. Maan, A. E. Rowan, R. J. M. Nolte, *Chem. Eur. J.* **2004**, *10*, 831.

[10] a) J. Tang, G. Ge, L. E. Brus, *J. Phys. Chem. B* **2002**, *106*, 5653–5658; E. Rabani, D. R. Reichman, P. L. Geissler, L. E. Brus, *Nature* **2003**, *426*, 271; b) E. Lauga, M. P. Brenner, *Phys. Rev. Lett.* **2004**, *93*, 238301.

[11] L. V. Govor, G. Reiter, J. Parisi, G. H. Bauer, *Phys. Rev. E* **2004**, *69*, 061609; L. V. Gover, G. Reiter, G. H. Bauer, J. Parisi, *Appl. Phys. Lett.* **2004**, *84*, 4774–4776.
[12] a) A. P. Sommer, M. Ben-Moshe, S. Magdassi, *J. Phys. Chem. B* **2004**, *108*, 8–10; X. Chen. Z. Chen, B. Yang, G. Zhang, J. Shen, *J. Colloid Interface Sci.* **2004**, *269*, 79–83; K. Chen, A. Taflove, Y. L. Kim, V. Backman, *Appl. Phys. Lett.* **2005**, *86*, 033101; b) H. Li, Q. Liu, L. Qin, M. Xu, X. Lin, S. Yin, L. Wu, Z. Su, J. Shen, *J. Colloid Interface Sci.* **2005**, *289*, 488–497.
[13] a) B. H. Hong, J. Y. Lee, C.-W. Lee, J. C. Kim, S. C. Bae, K. S. Kim, *J. Am. Chem. Soc.* **2001**, *123*, 10748–10749; b) S. Leclair, P. Baillargeon, R. Skouta, D. Gauthier, Y. Zhao, Y. L. Dory, *Angew. Chem.* **2004**, *116*, 353–357; *Angew. Chem. Int. Ed.* **2004**, *43*, 349–353; S. Leclair, P. Baillargeon, R. Skouta, D. Gauthier, Y. Zhao, Y. L. Dory, *Angew. Chem.* **2004**, *116*, 353–357; c) J.-S. Hu, Y.-G. Guo, H.-P. Liang, L.-J. Wan, L. Jiang, *J. Am. Chem. Soc.* **2005**, *127*, 17090–17095.
[14] a) H. Nakamura, Y. Matsui, *J. Am. Chem. Soc.* **1995**, *117*, 2651–2652; F. Miyaji, S. A. Davis, J. P. H. Charmant, S. Mann, *Chem. Mater.* **1999**, *11*, 3021–3024; b) F. Mallet, S. Petit, S. Lafont, P. Billot, D. Lemarchand, G. Coquerel, *Cryst. Growth Des.* **2004**, *4*, 965–969.

